Status of the Bonn-Gatchina partial wave analysis

A. Anisovich

HISKP, Uni-Bonn (Bonn) and PNPI (Gatchina)

HISKP

Petersburg
Nuclear
Physics
Institute

Topics

- **Data review**
- **Multipole decomposition of the single pion photoproduction amplitude**
- $P_{11}(1/2^+)$ **wave**
- $P_{13}(3/2^+)$ **wave**

Bonn-Gatchina PWA group

A. Anisovich, E. Klempt, V. Nikonov, A. Sarantsev and U. Thoma.

Aims of BnGa PWA

- **Aim: Determination of the full spectrum of baryon resonances and their decay modes**
- **Method: Simultaneous description of all relevant data for baryon spectroscopy**

Pion induced reactions with recently included data sets.

Observable	$N_{\rm data}$	$\frac{\chi^2}{N_{\rm data}}$		Observable	$N_{\rm data}$	$\frac{\chi^2}{N_{\rm data}}$	
$N^*_{1/2-}$ $S_{11}(\pi N \to \pi N)$	**104**	**1.81**	**SAID**	$\Delta_{1/2-}$ $S_{31}(\pi N \to \pi N)$	**112**	**2.27**	**SAID**
$N^*_{1/2+}$ $P_{11}(\pi N \to \pi N)$	**112**	**2.49**	**SAID**	$\Delta_{1/2+}$ $P_{31}(\pi N \to \pi N)$	**104**	**2.01**	**SAID**
$N^*_{3/2+}$ $P_{13}(\pi N \to \pi N)$	**112**	**1.90**	**SAID**	$\Delta^*_{3/2+}$ $P_{33}(\pi N \to \pi N)$	**120**	**2.53**	**SAID**
$\Delta^*_{3/2-}$ $D_{33}(\pi N \to \pi N)$	**108**	**2.56**	**SAID**	$N^*_{3/2-}$ $D_{13}(\pi N \to \pi N)$	**96**	**2.16**	**SAID**
$N^*_{5/2-}$ $D_{15}(\pi N \to \pi N)$	**96**	**3.37**	**SAID**	$\Delta_{5/2+}$ $F_{35}(\pi N \to \pi N)$	**62**	**1.32**	**SAID**
$\Delta_{7/2+}$ $F_{37}(\pi N \to \pi N)$	**72**	**2.86**	**SAID**				
$d\sigma/d\Omega(\pi^- p \to n\eta)$	**70**	**1.96**	**Richards *et al.***	$d\sigma/d\Omega(\pi^- p \to n\eta)$	**84**	**2.67**	**CBALL**
$d\sigma/d\Omega(\pi^- p \to K\Lambda)$	**479**	**1.55**	**RAL**	$P(\pi^- p \to K\Lambda)$	**261**	**1.76**	**RAL+ANL**
$d\sigma/d\Omega(\pi^+ p \to K^+\Sigma)$	**609**	**1.91**	**RAL**	$P(\pi^+ p \to K^+\Sigma)$	**420**	**2.74**	**RAL**
$d\sigma/d\Omega(\pi^- p \to n\pi^0\pi^0)$			**CBALL**				

Single meson photoproduction reactions with recently included data sets.

Observable	$N_{\rm data}$	$\frac{\chi^2}{N_{\rm data}}$		Observable	$N_{\rm data}$	$\frac{\chi^2}{N_{\rm data}}$	
$d\sigma/d\Omega(\gamma p \to p\pi^0)$	1106	1.34	CB-ELSA	$d\sigma/d\Omega(\gamma p \to p\pi^0)$	861	1.46	GRAAL
$d\sigma/d\Omega(\gamma p \to p\pi^0)$	592	2.11	CLAS	$d\sigma/d\Omega(\gamma p \to p\pi^0)$	1692	1.25	TAPS@MAMI
$E(\gamma p \to p\pi^0)$	140	1.23	A2-GDH	$\Sigma(\gamma p \to p\pi^0)$	1492	3.26	SAID db
$P(\gamma p \to p\pi^0)$	607	3.23	SAID db	$T(\gamma p \to p\pi^0)$	389	3.71	SAID db
$H(\gamma p \to p\pi^0)$	71	1.26	SAID db	$G(\gamma p \to p\pi^0)$	75	1.50	SAID db
$O_x(\gamma p \to p\pi^0)$	7	1.77	SAID db	$O_z(\gamma p \to p\pi^0)$	7	0.46	SAID db
$d\sigma/d\Omega(\gamma p \to n\pi^+)$	1583	1.64	SAID db	$d\sigma/d\Omega(\gamma p \to n\pi^+)$	408	0.62	A2-GDH
$\Sigma(\gamma p \to n\pi^+)$	899	3.48	SAID db	$E(\gamma p \to n\pi^+$	231	1.55	A2-GDH
$P(\gamma p \to n\pi^+)$	252	2.90	SAID db	$T(\gamma p \to n\pi^+)$	661	3.21	SAID db
$H(\gamma p \to p\pi^+)$	71	3.90	SAID db	$G(\gamma p \to p\pi^+)$	86	5.64	SAID db
$d\sigma/d\Omega(\gamma p \to p\eta)$	680	1.47	CB-ELSA	$d\sigma/d\Omega(\gamma p \to p\eta)$	100	2.16	TAPS
$\Sigma(\gamma p \to p\eta)$	51	2.26	GRAAL 98	$\Sigma(\gamma p \to p\eta)$	100	2.02	GRAAL 07
$T(\gamma p \to p\eta)$	50	1.48	Phoenics				

Comparison of different data sets on the $\gamma p \to \pi^0 p$ differential cross section, curve represents preliminary fit.

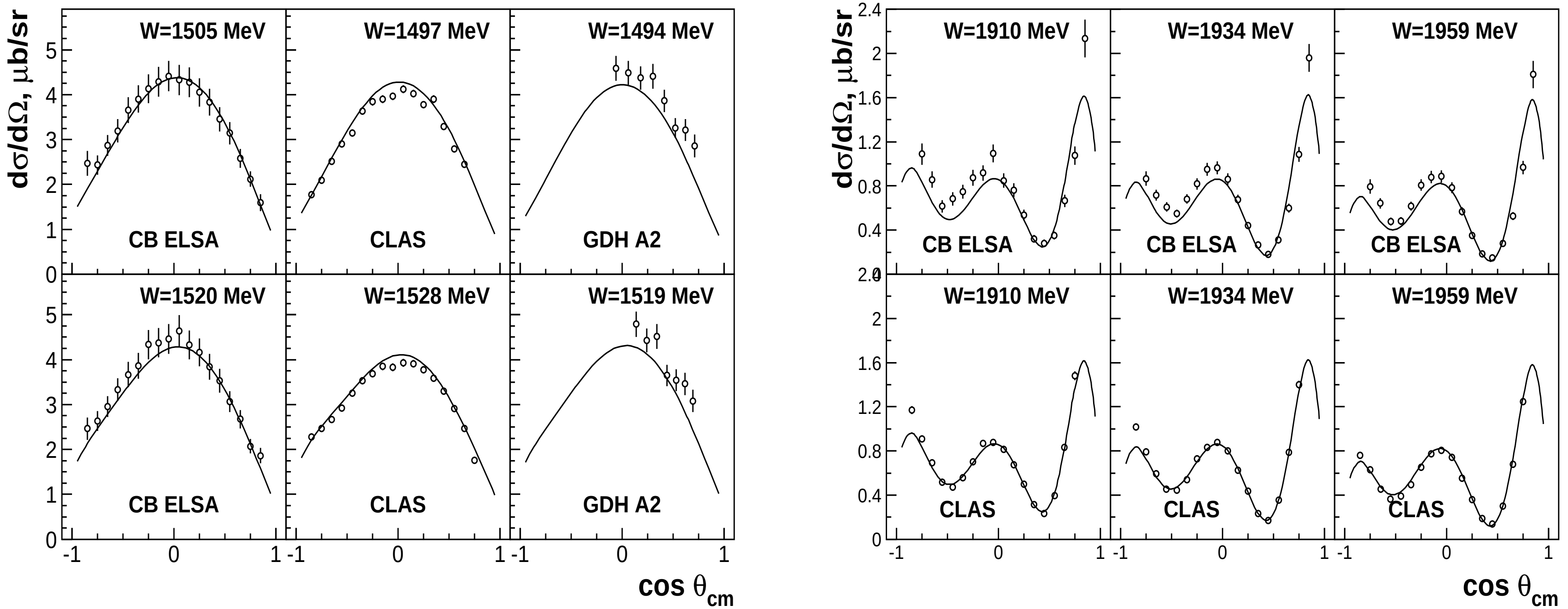

1. **Free normalization factors (0.95-1.05) for each data sets are used;**
2. **Additional systematic errors are estimated and used in the fit**

The fitted reactions. Recently included data sets.

Observable	$N_{\rm data}$	$\frac{\chi^2}{N_{\rm data}}$		Observable	$N_{\rm data}$	$\frac{\chi^2}{N_{\rm data}}$	
$C_x(\gamma p\to \Lambda K^+)$	160	1.23	CLAS	$C_x(\gamma p\to \Sigma^0 K^+)$	94	2.20	CLAS
$C_z(\gamma p\to \Lambda K^+)$	160	1.41	CLAS	$C_z(\gamma p\to \Sigma^0 K^+)$	94	2.00	CLAS
$d\sigma/d\Omega(\gamma p\to \Lambda K^+)$	1377	1.81	CLAS	$d\sigma/d\Omega(\gamma p\to \Sigma^0 K^+)$	1280	2.06	CLAS
$P(\gamma p\to \Lambda K^+)$	202	2.03	CLAS	$P(\gamma p\to \Sigma^0 K^+)$	95	1.45	CLAS
$\Sigma(\gamma p\to \Lambda K^+)$	66	1.53	GRAAL	$\Sigma(\gamma p\to \Sigma^0 K^+)$	42	0.90	GRAAL
$\Sigma(\gamma p\to \Lambda K^+)$	45	1.65	LEP	$\Sigma(\gamma p\to \Sigma^0 K^+)$	45	1.11	LEP
$T(\gamma p\to \Lambda K^+)$	66	1.26	GRAAL 09	$d\sigma/d\Omega(\gamma p\to \Sigma^+ K^0)$	48	3.76	CLAS
$O_x(\gamma p\to \Lambda K^+)$	66	1.30	GRAAL 09	$d\sigma/d\Omega(\gamma p\to \Sigma^+ K^0)$	160	0.98	CB-ELSA
$O_z(\gamma p\to \Lambda K^+)$	66	1.54	GRAAL 09	$P(\gamma p\to \Sigma^+ K^0)$	72	0.61	CB-ELSA
$d\sigma/d\Omega(\gamma p\to p\pi^0\pi^0)$	CB-ELSA (1.4 GeV)			$E(\gamma p\to p\pi^0\pi^0)$	16	1.91	MAMI
$d\sigma/d\Omega(\gamma p\to p\pi^0\eta)$	CB-ELSA (3.2 GeV)			$\Sigma(\gamma p\to p\pi^0\eta)$	180	2.37	GRAAL
$d\sigma/d\Omega(\gamma p\to p\pi^0\pi^0)$	CB-ELSA (3.2 GeV)			$\Sigma(\gamma p\to p\pi^0\pi^0)$	128	0.96	GRAAL

$\gamma p \to \pi^0 p$ from Crystal Barrel at ELSA ($E_\gamma \leq 3.2$ GeV)

$\Delta(1232)P_{33}$
$N(1520)D_{13}$
$N(1535)S_{11}$
$N(1650)S_{11}$
$N(1680)F_{15}$
$\Delta(1700)D_{33}$
$\Delta(1920)P_{33}$

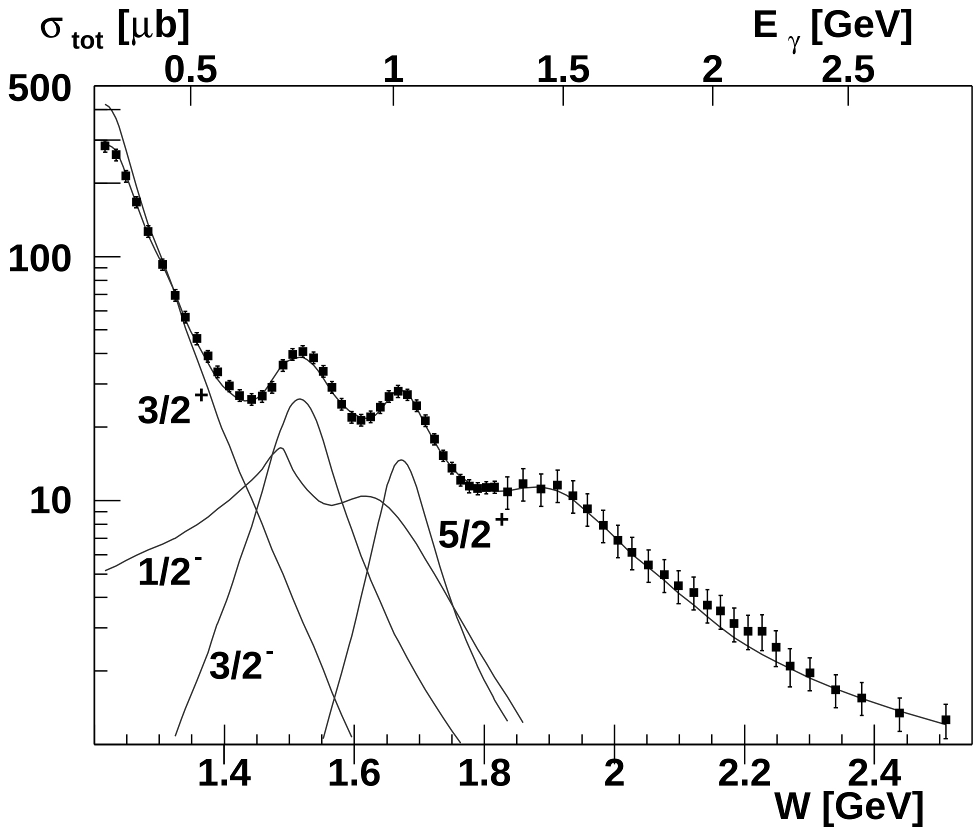

CLAS 07 data on the differential cross section for $\gamma p \to \pi^0 p$ with current solution. Only statistical errors for the CLAS data are shown.

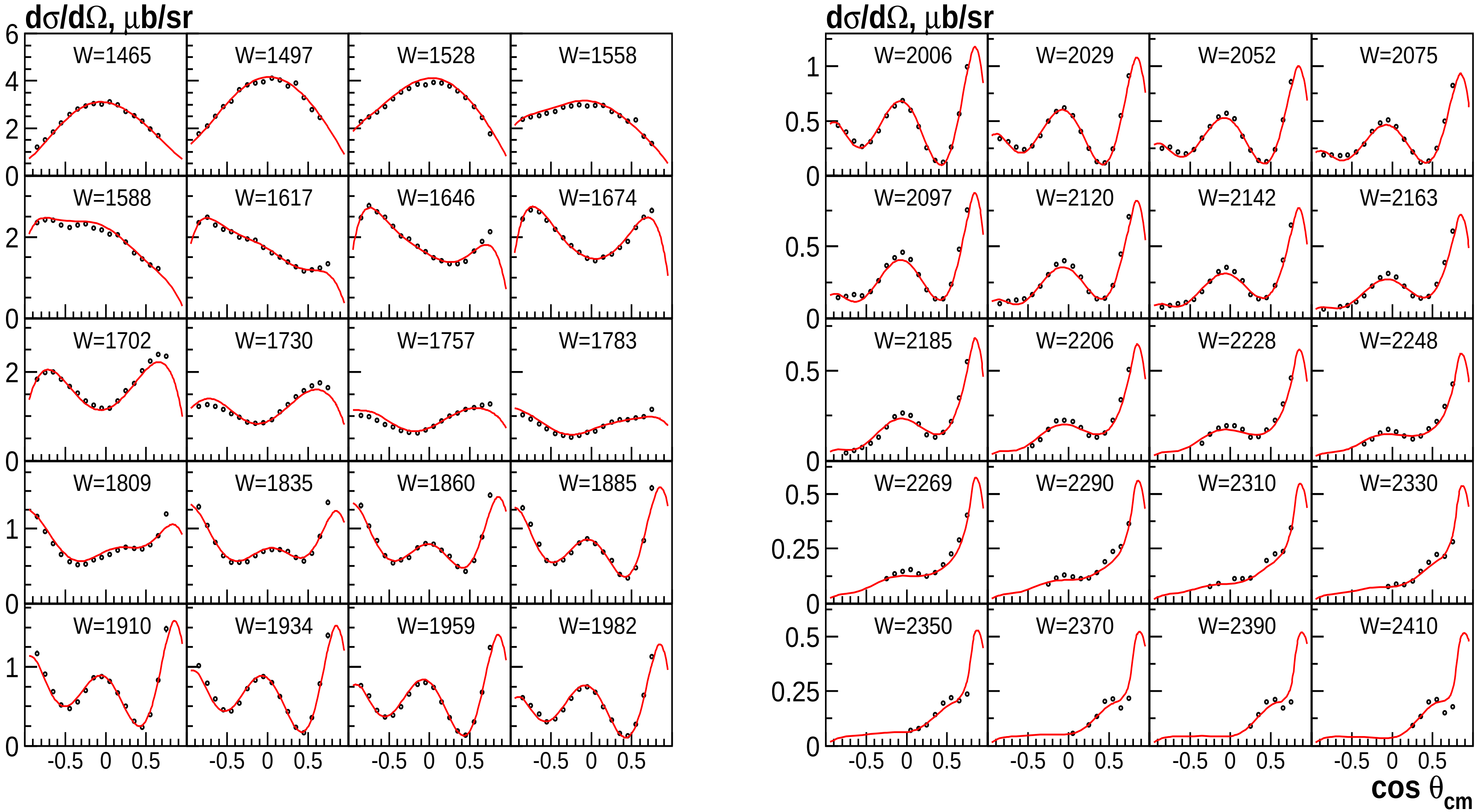

CLAS 09 data on the differential cross section for $\gamma p \to \pi^+ n$ with current solution.

Only statistical errors for the CLAS data are shown.

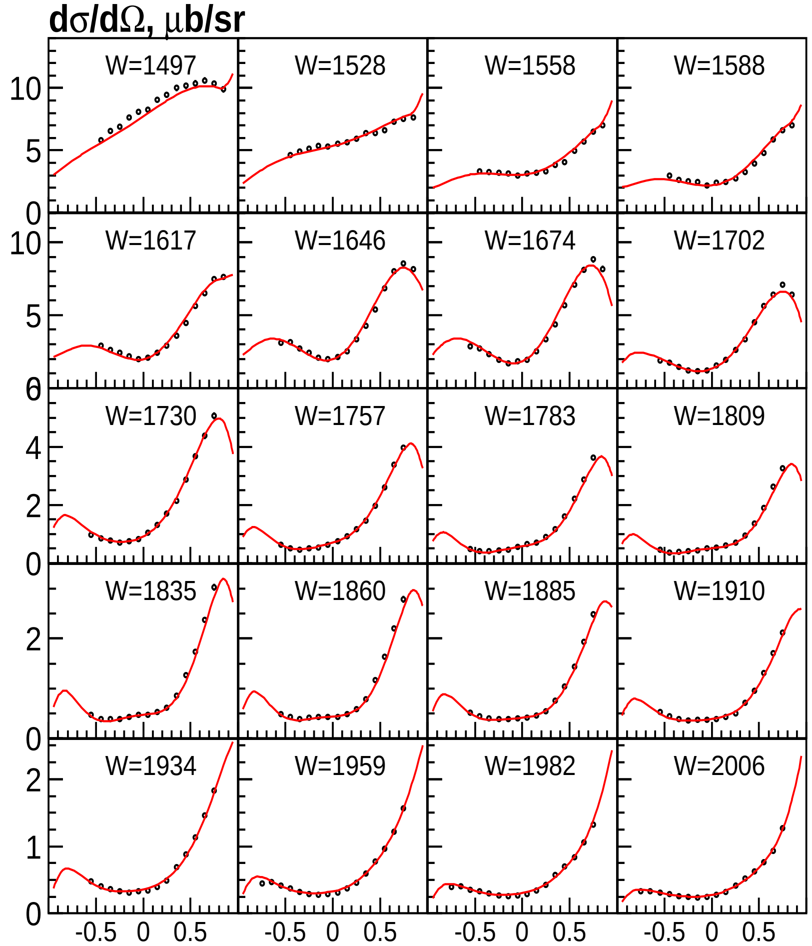

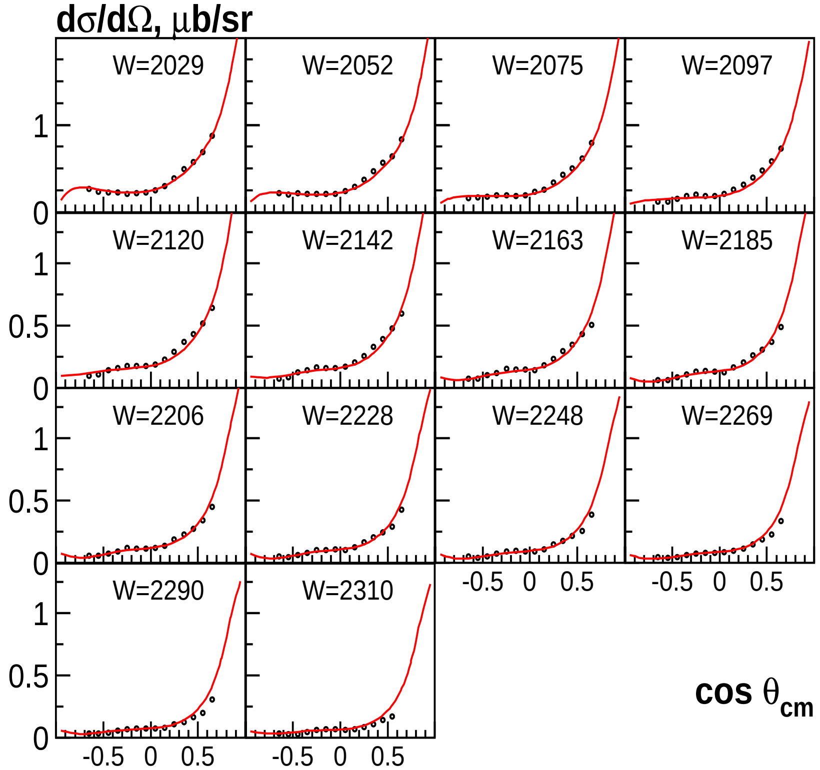

Photoproduction multipoles and partial waves. In general, two multipoles lead to one spin-parity wave.

Multipoles		Partial waves		J^P
E_0^+	-	S_{11}	S_{31}	$1/2^-$
-	M_1^-	P_{11}	P_{31}	$1/2^+$
E_1^+	M_1^+	P_{13}	P_{33}	$3/2^+$
E_2^-	M_2^-	D_{13}	D_{33}	$3/2^-$
E_2^+	M_2^+	D_{15}	D_{35}	$5/2^-$
E_3^-	M_3^-	F_{15}	F_{35}	$5/2^+$

Real (left) and imaginary (right) parts of multipoles for the π^0 photoproduction.

Red - BoGa solution, blue - SAID, MAID 2009.

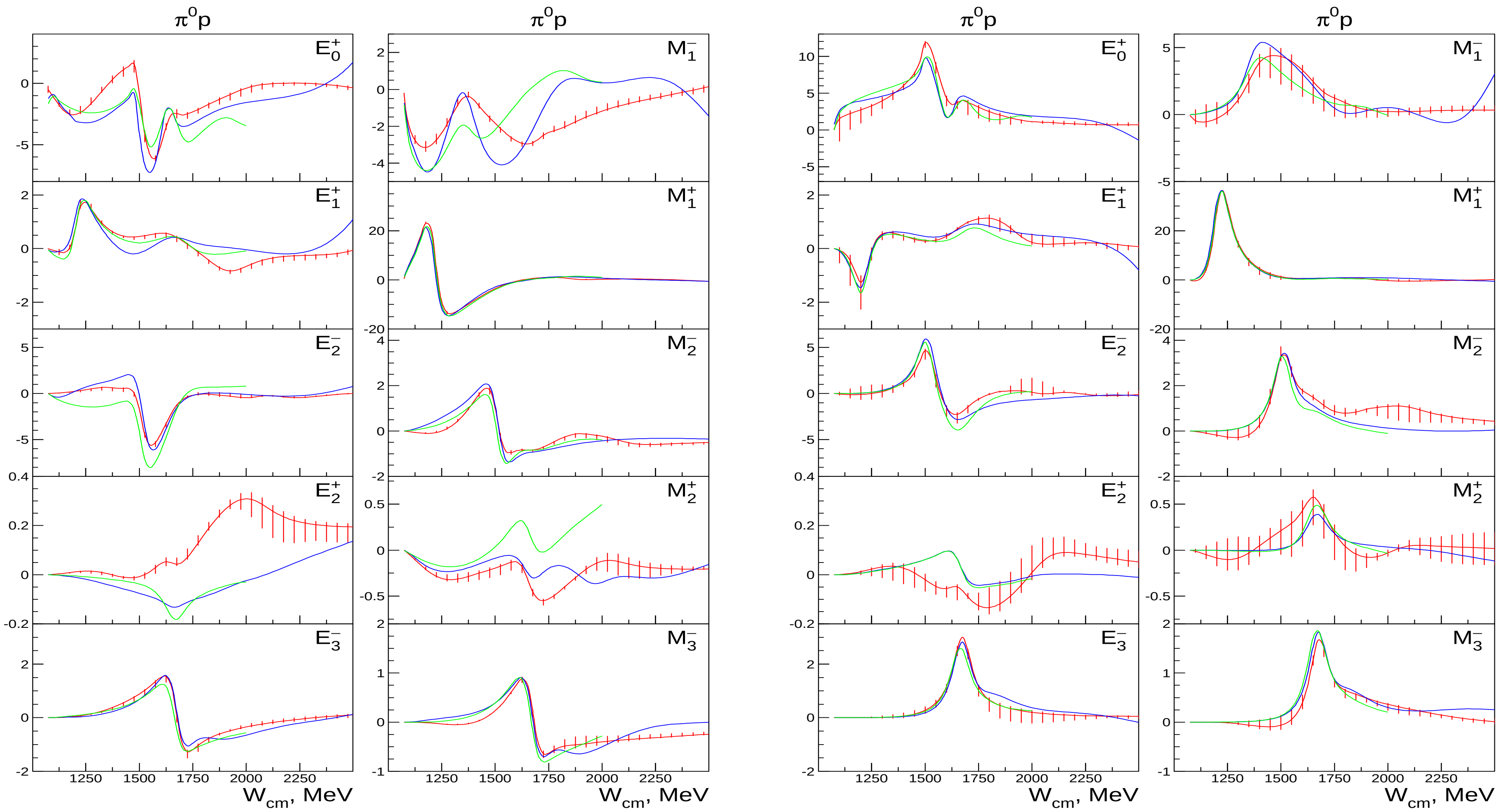

Real (left) and imaginary (right) parts of multipoles for the π^+ photoproduction.

Red - BoGa solution, blue - SAID, MAID 2009.

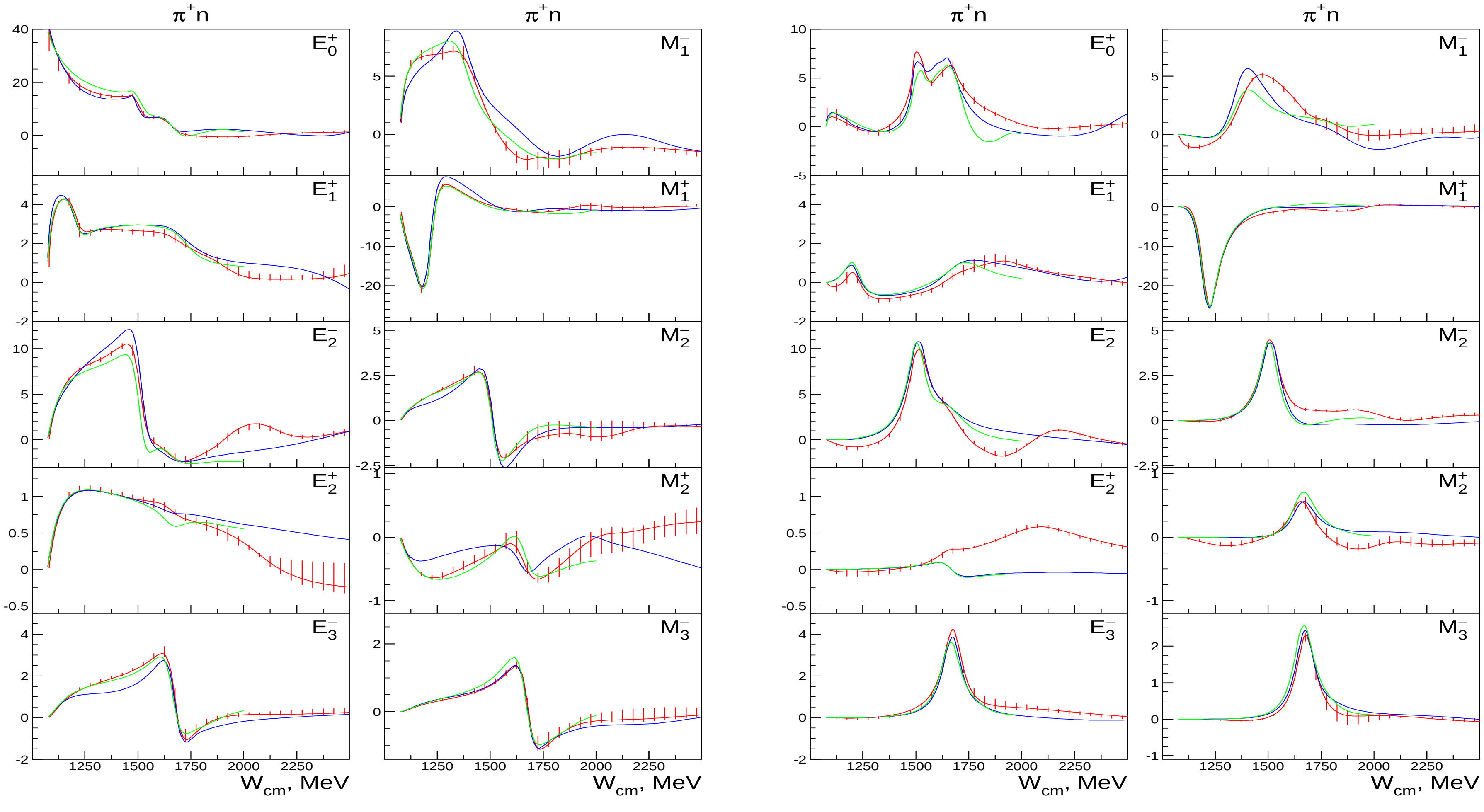

$N\pi \to N\pi\ P_{11}$ wave (3 pole 4 channel K-matrix)

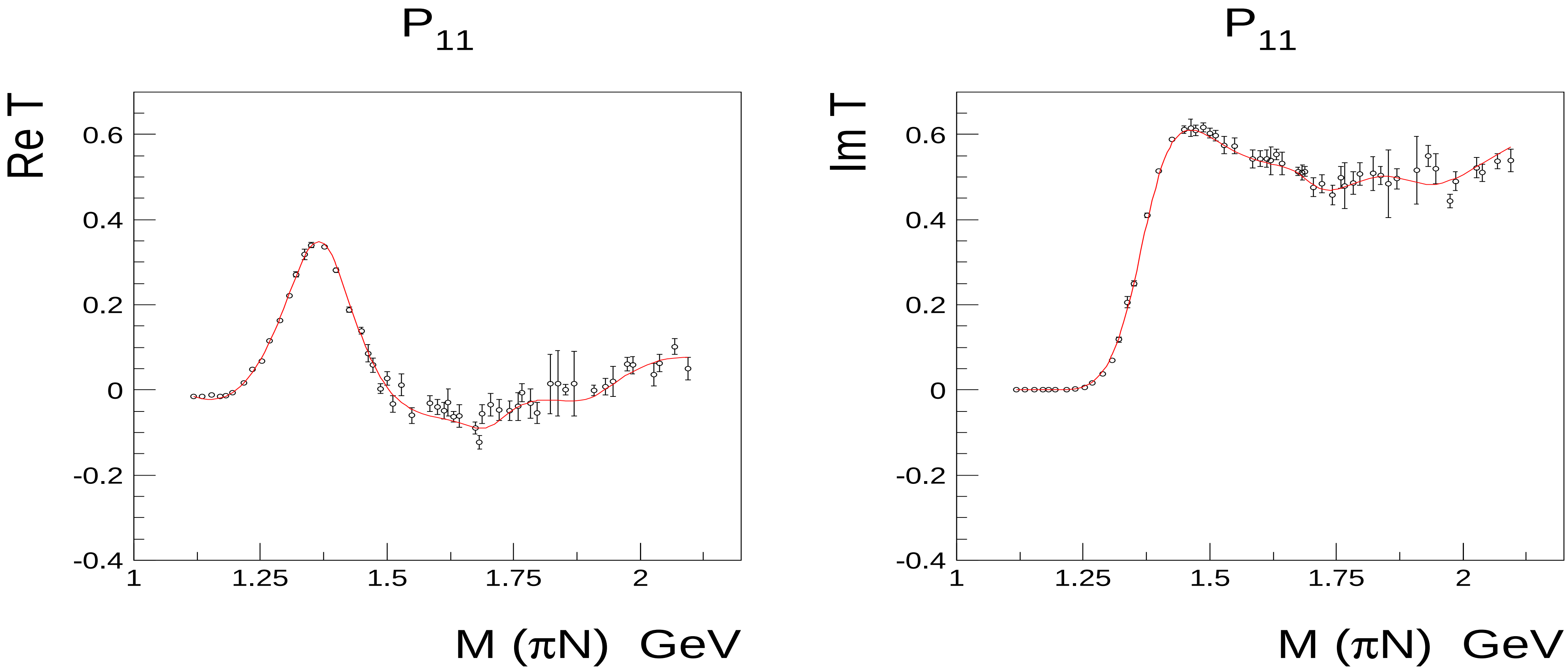

T-matrix poles (our fit and PDG value):

$M = 1370 \pm 4$ **(**1365 ± 15**) MeV,** $-2\ Im = 193 \pm 7$ **(**190 ± 30**) MeV;**

$M = 1708 \pm 18$ **(**1720 ± 50**) MeV,** $-2\ Im = 200 \pm 20$ **(**230 ± 150**)MeV;**

$M = 1870 \pm 30$ **MeV,** $-2\ Im = 280 \pm 80$ **MeV**

$\pi^- p \to n\pi^0\pi^0$ (Crystal Ball) total cross section

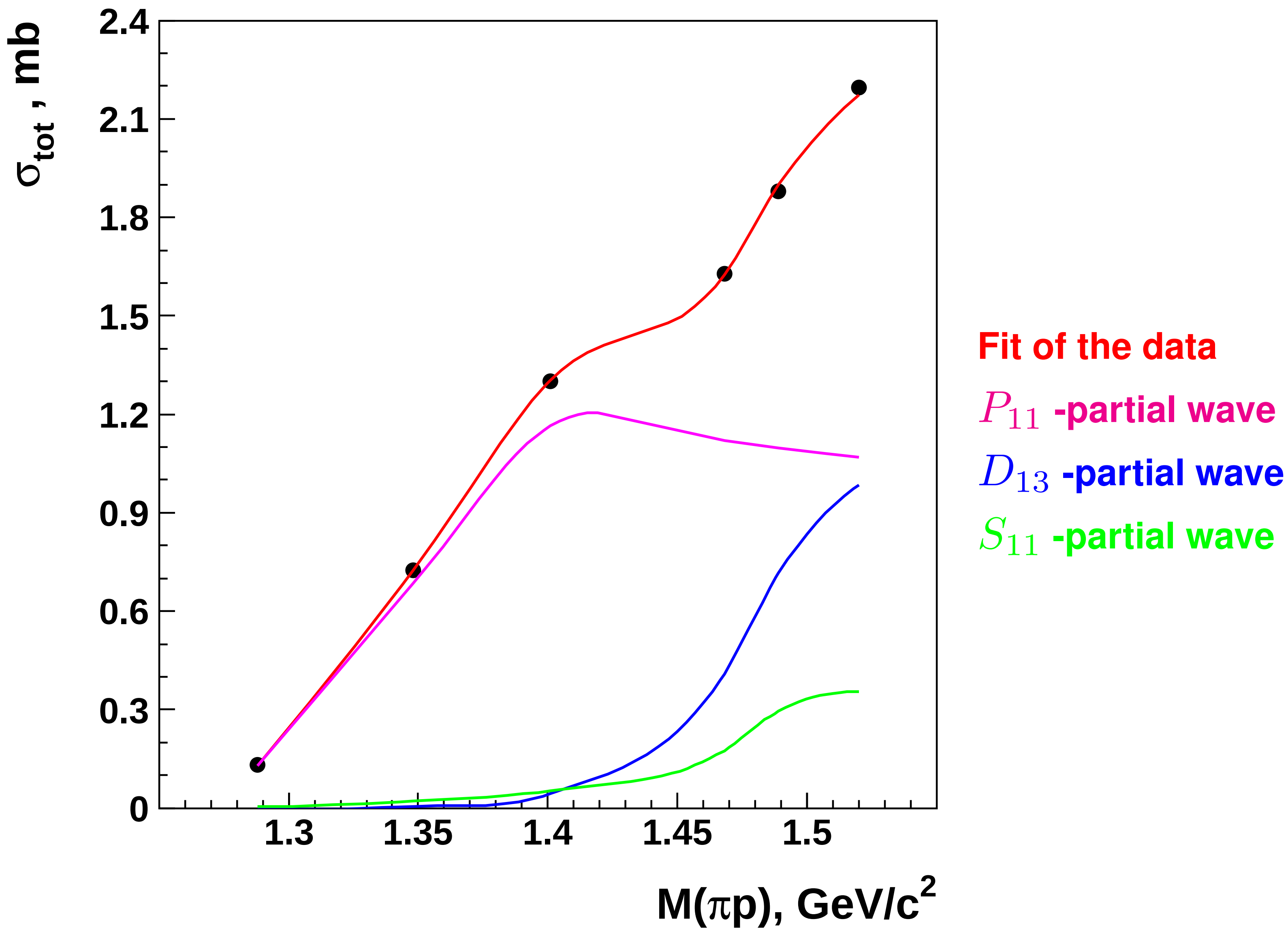

$\gamma p \to p\pi^0\pi^0$ (CB-ELSA) M.Fuchs et al.

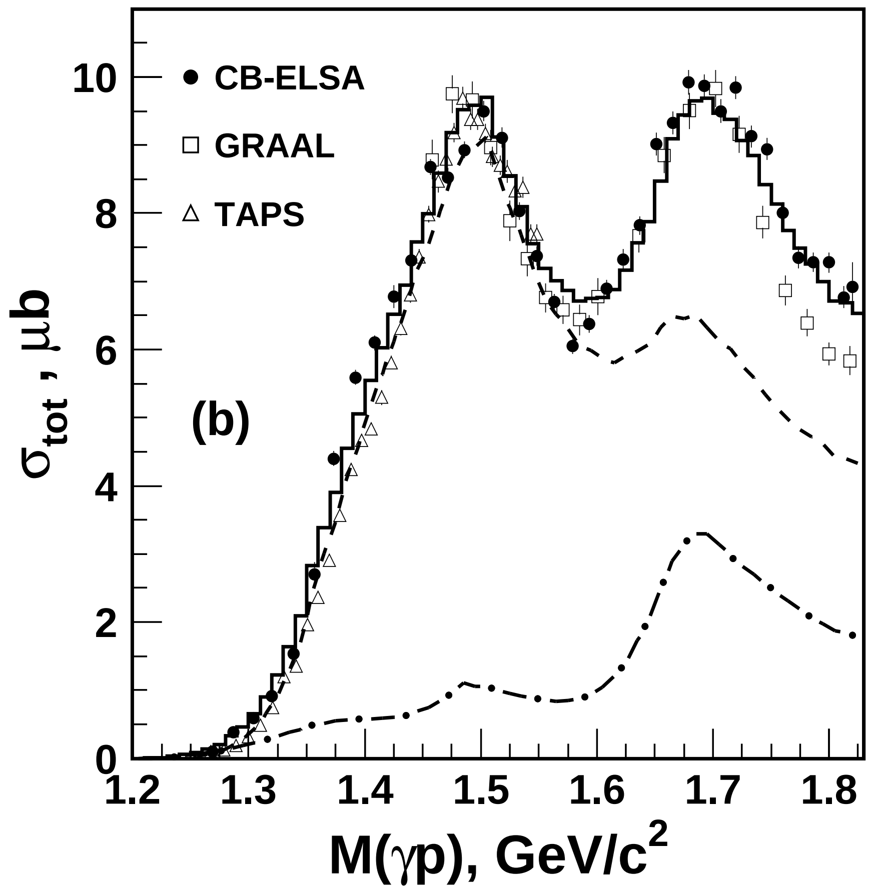

PWA corrected cross section and contributions from $\Delta(1232)\pi$ (dashed) and $N\sigma$ (dashed-dotted) final states.

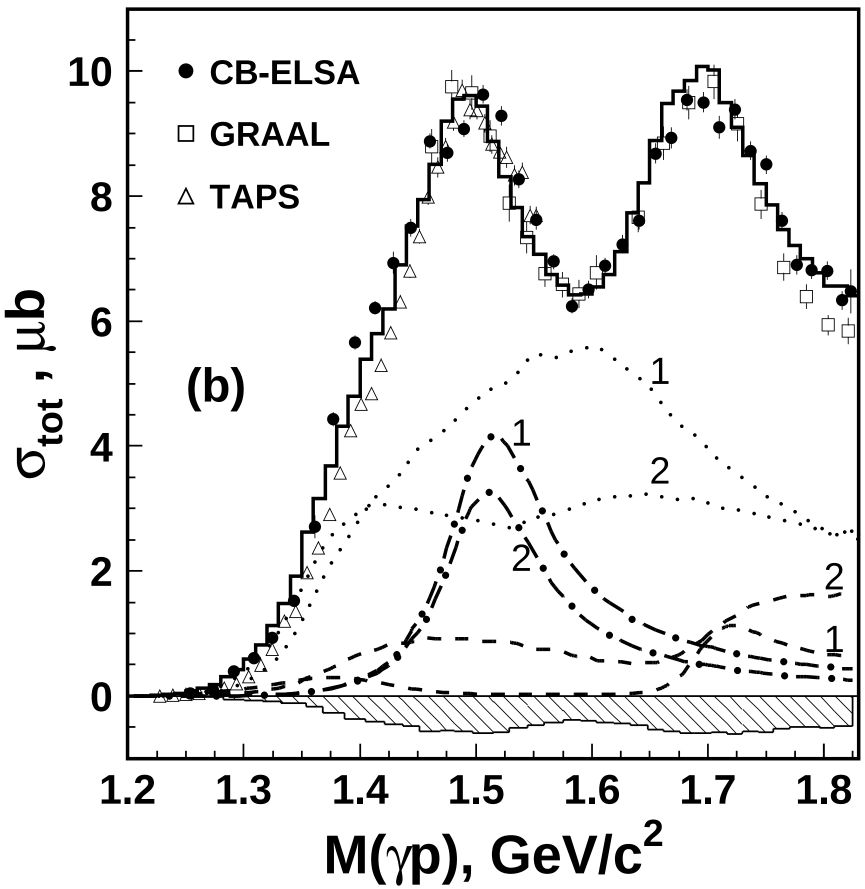

Contributions from D_{33} (dotted), P_{11} (dashed) and D_{13} (dashed-dotted) partial waves.

The $\gamma p \to \pi^0\pi^0 p$ helicity $3/2$ and $1/2$ differential cross sections

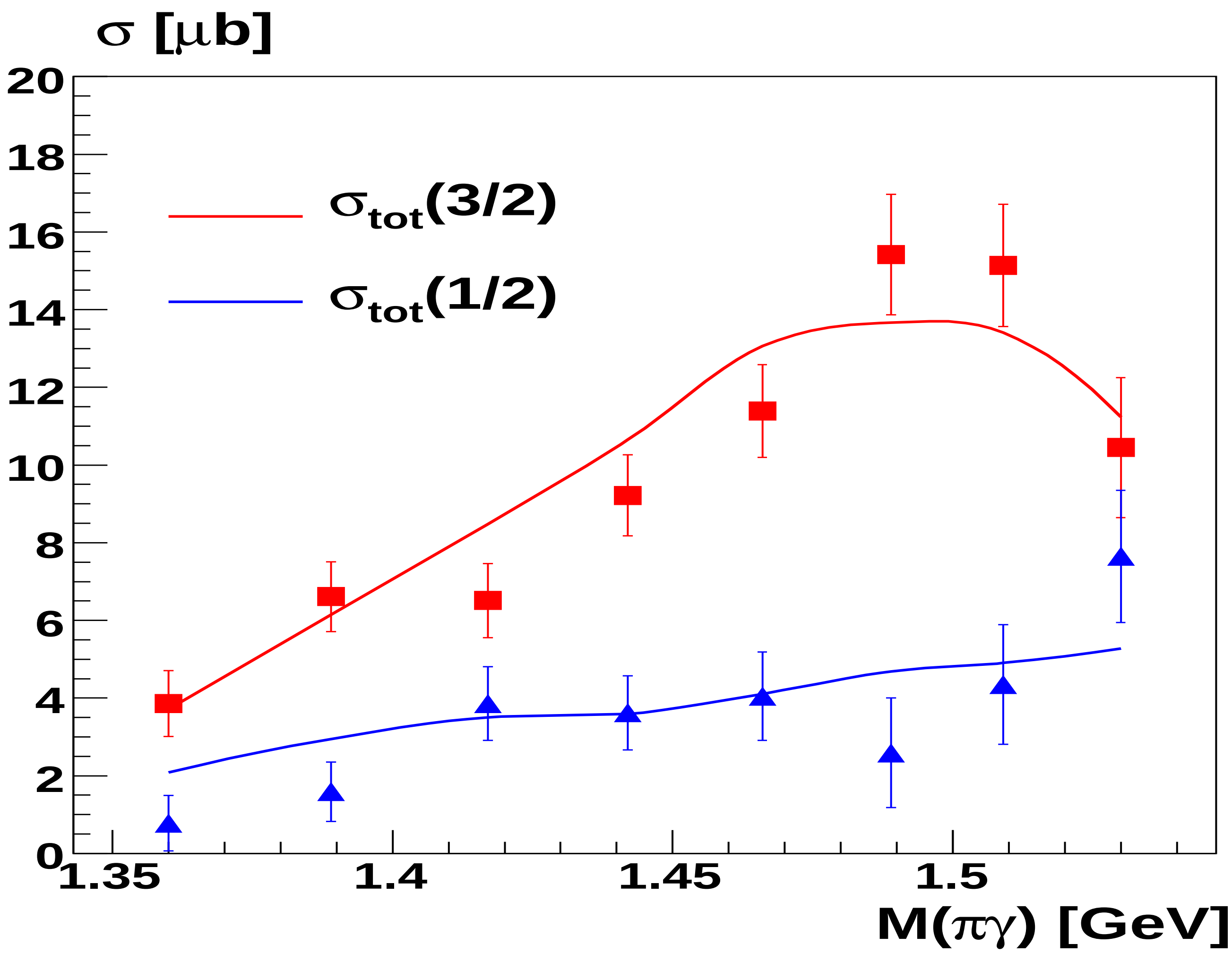

Properties of $N(1440)P_{11}$. The left column lists mass, width, partial widths of the Breit-Wigner resonance; the right column stands for pole position and squared couplings to the final state at the pole position.

M	=	1436 ± 15 MeV	M$_{\rm pole}$	=	1371 ± 7 MeV
Γ	=	335 ± 40 MeV	$\Gamma_{\rm pole}$	=	192 ± 20 MeV
$\Gamma_{\pi N}$	=	205 ± 25 MeV	$g_{\pi N}$	=	$(0.51 \pm 0.05) \cdot e^{-i\pi\frac{(35\pm5)}{180}}$
$\Gamma_{\sigma N}$	=	71 ± 17 MeV	$g_{\sigma N}$	=	$(0.82 \pm 0.16) \cdot e^{-i\pi\frac{(20\pm13)}{180}}$
$\Gamma_{\pi\Delta}$	=	59 ± 15 MeV	$g_{\pi\Delta}$	=	$(-0.57 \pm 0.08) \cdot e^{i\pi\frac{(25\pm20)}{180}}$
T-matrix: $A_{1/2} = 0.055 \pm 0.020$ GeV			$\phi = (70 \pm 30)^\circ$		

$P_{11}(1710)$ resonance

The differential cross section for the $\pi^- p \to K\Lambda$ reaction shows a clear contribution from this state ($S_{11} - P_{11}$ interference):

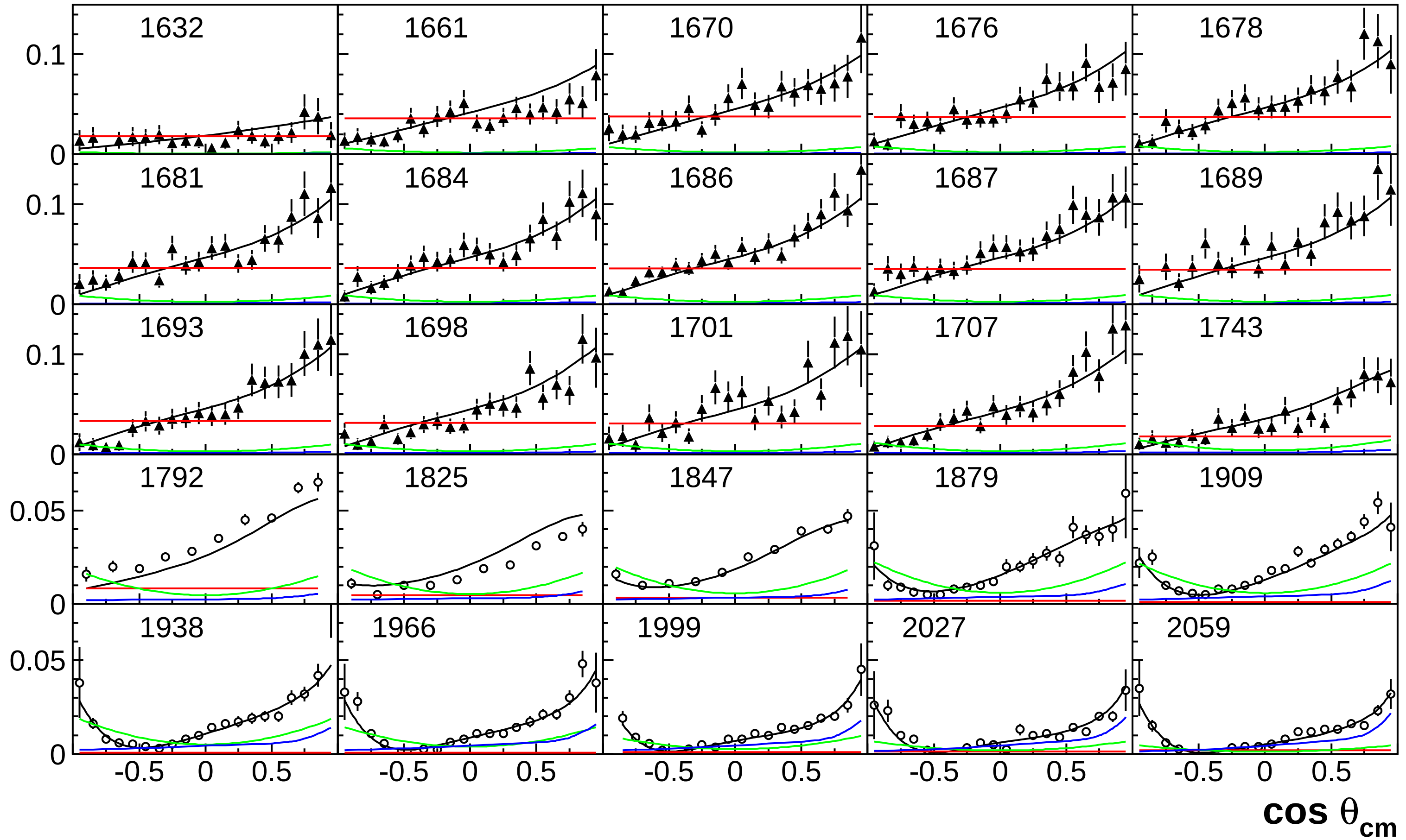

Preliminary fit

$P_{11}(1710)$ resonance

The total cross section for the $\pi^- p \to K\Lambda$ reaction:

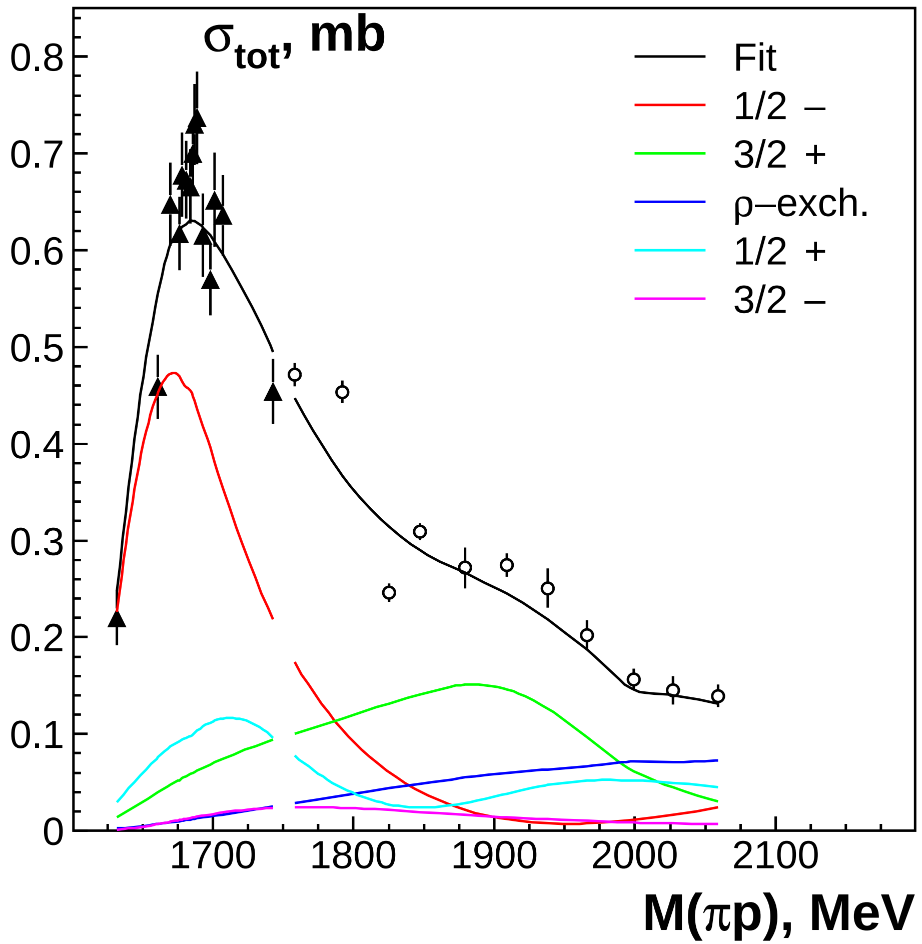

Preliminary result

$P_{11}(1710)$ resonance

The recoil asymmetry for the $\pi^- p \to K\Lambda$ reaction. also shows a clear contribution from this state:

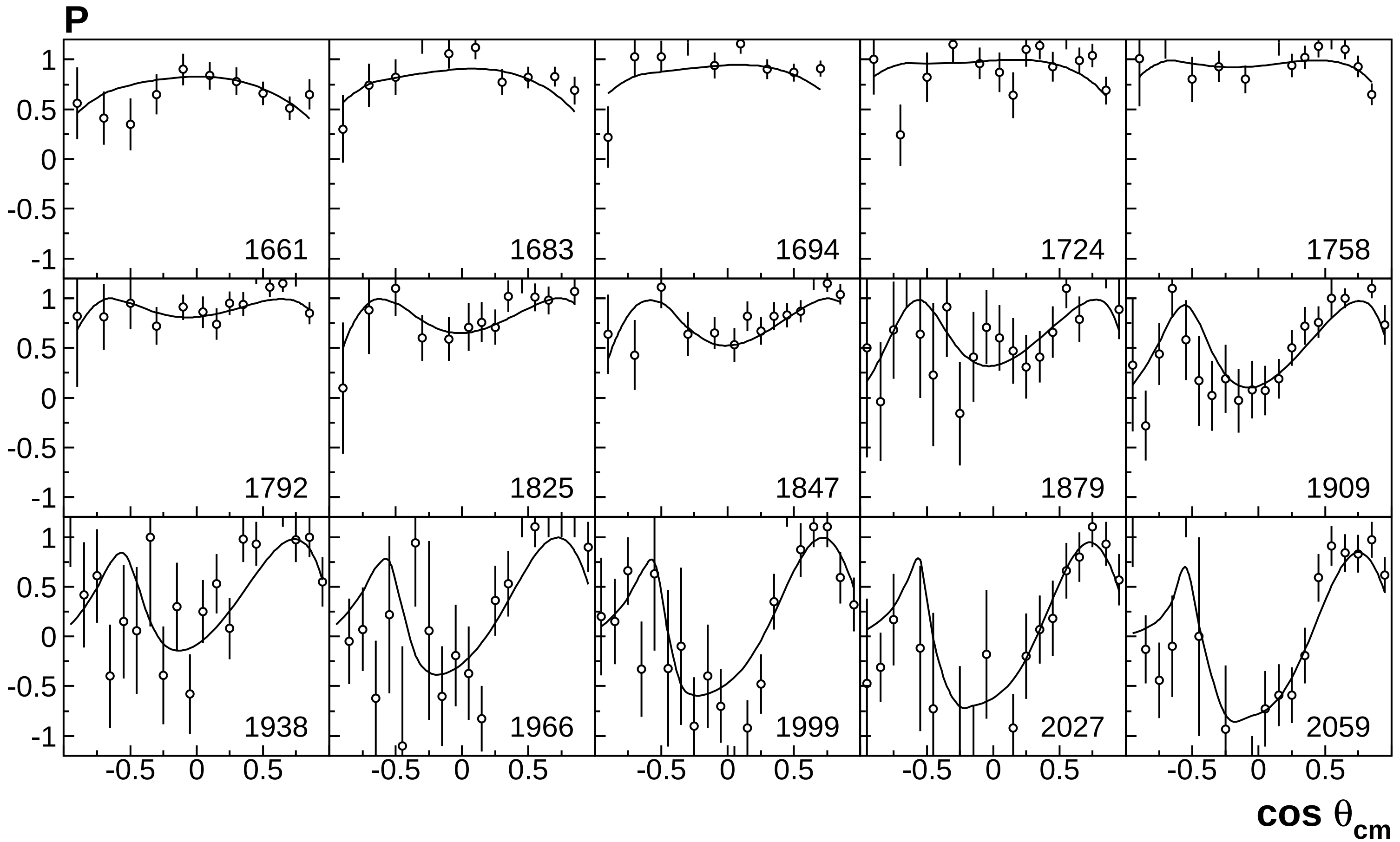

Preliminary fit

$P_{11}(1710)$ resonance

The data on $\pi^- p \to \eta n$ and the target asymmetry $\gamma p \to \eta p$ fix the position and couplings of $P_{11}(1710)$ state and reduce ηN coupling of the $P_{13}(1720)$ state.

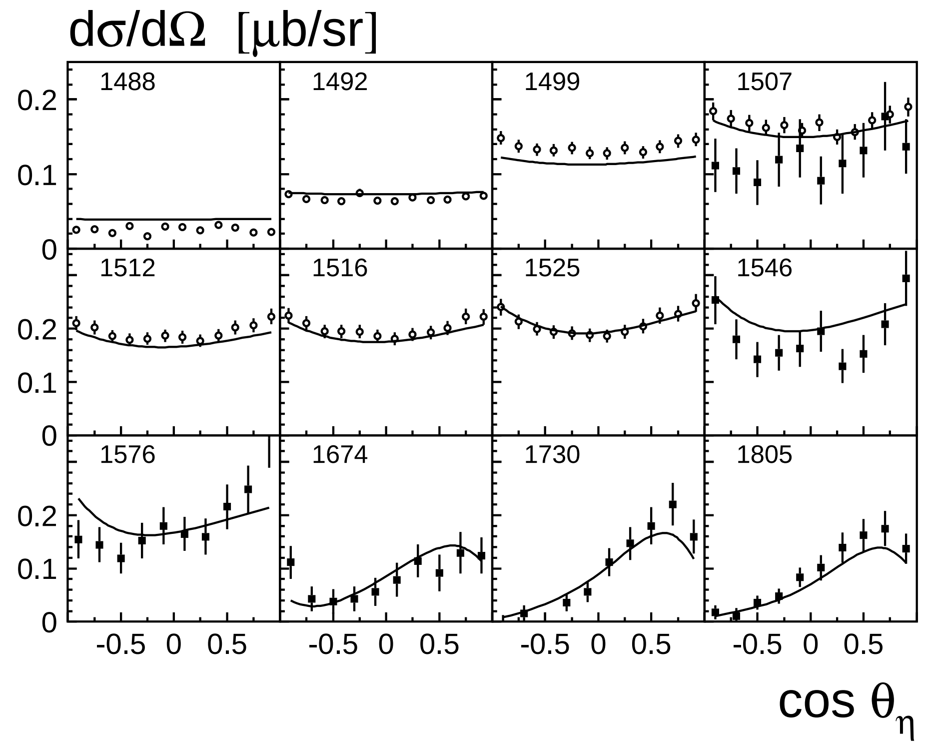

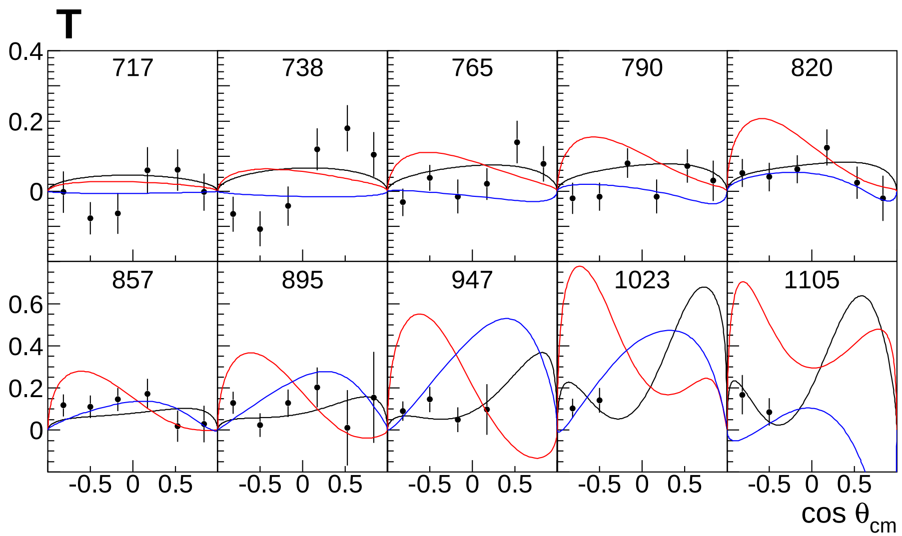

$\mathrm{N}\pi \to \mathrm{N}\pi$, P_{13} wave (3 pole 8 channel K-matrix)

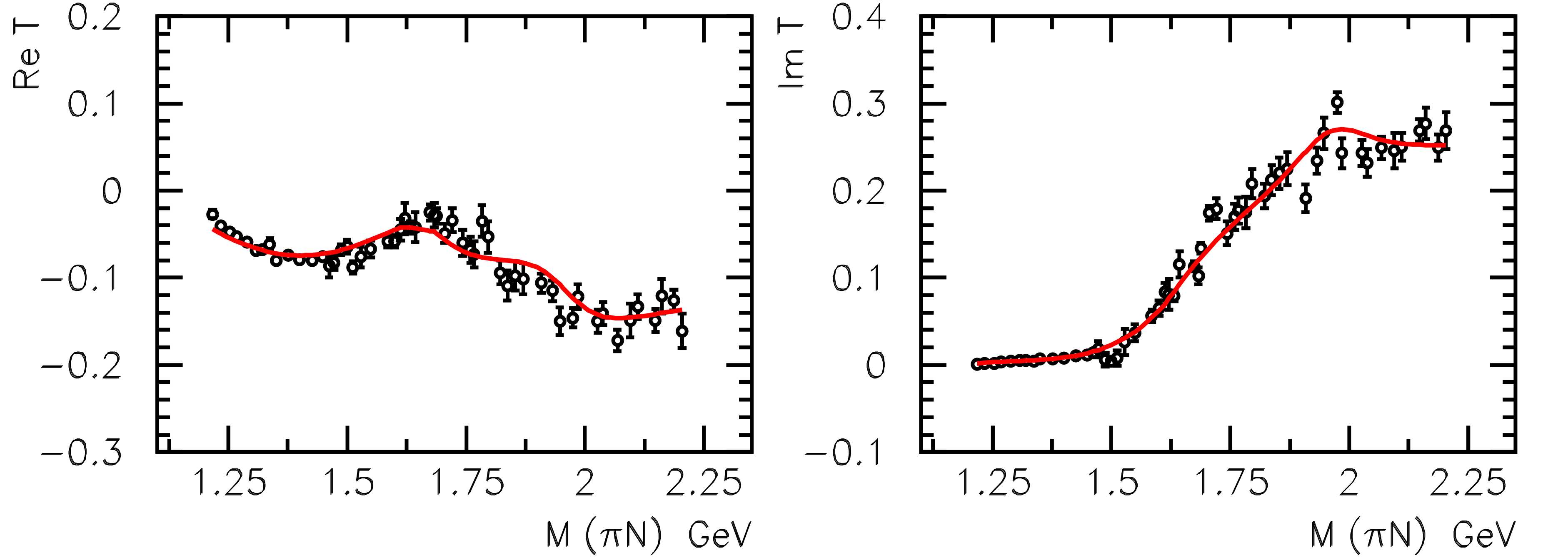

2nd T-matrix poles: $M = 1960 \pm 20$ **MeV,** $2\ Im = 195 \pm 45$ **MeV;**

$P_{13}(1900)$ resonance

For $\gamma p \to K\Lambda$ (left) and $\gamma p \to K\Sigma$ (right) we have almost complete photoproduction experiment: σ (CLAS, SAPHIR), Σ (GRAAL, LEP), P (CLAS), C_x, C_z (CLAS), T, O_x, O_z (GRAAL).

The C_x and C_z data can be explained with $P_{13}(1900)$.

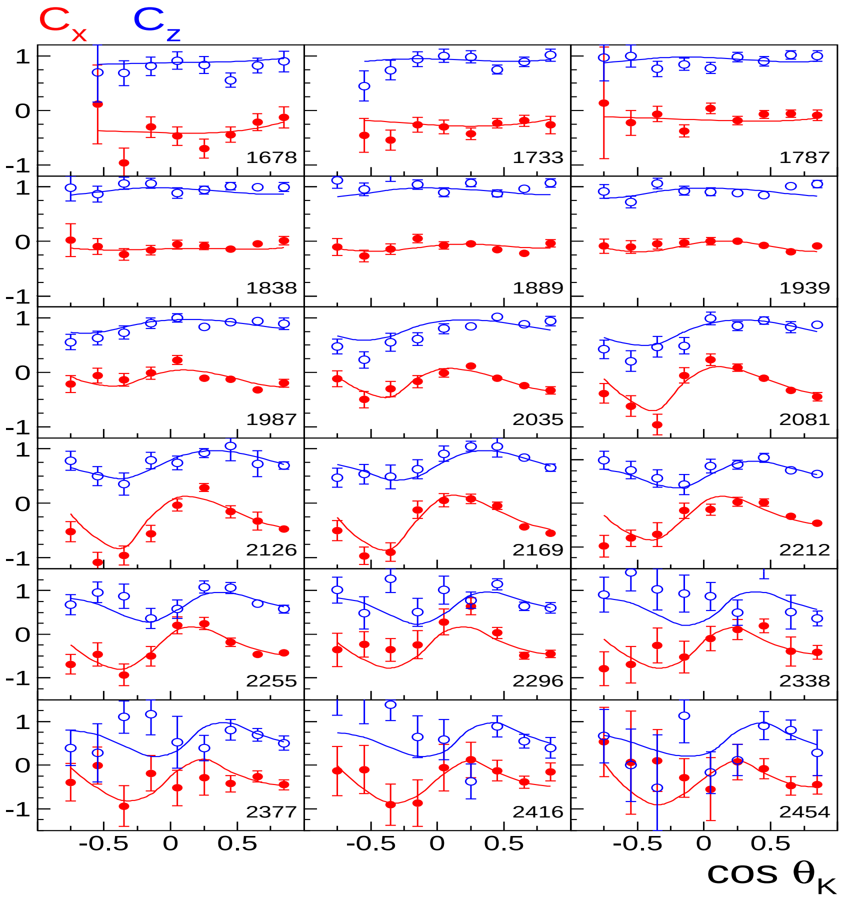

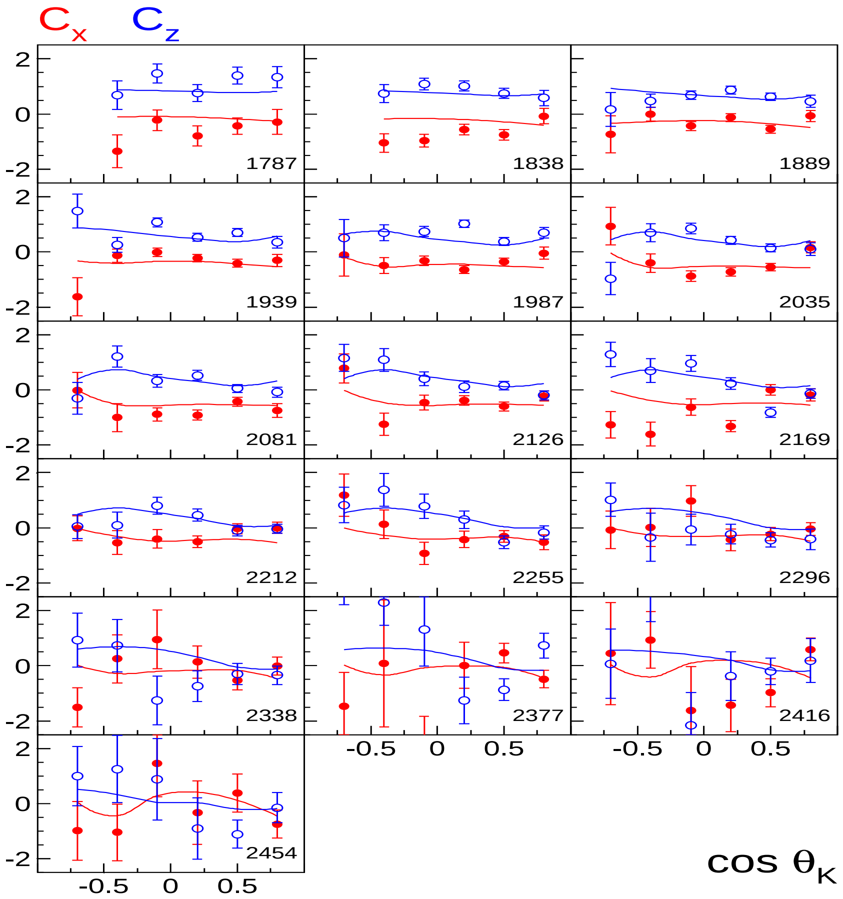

$P_{13}(1900)$ resonance

The solution is supported by the new GRALL data on O_x O_z and T-observables: an important step to a complete experiment.

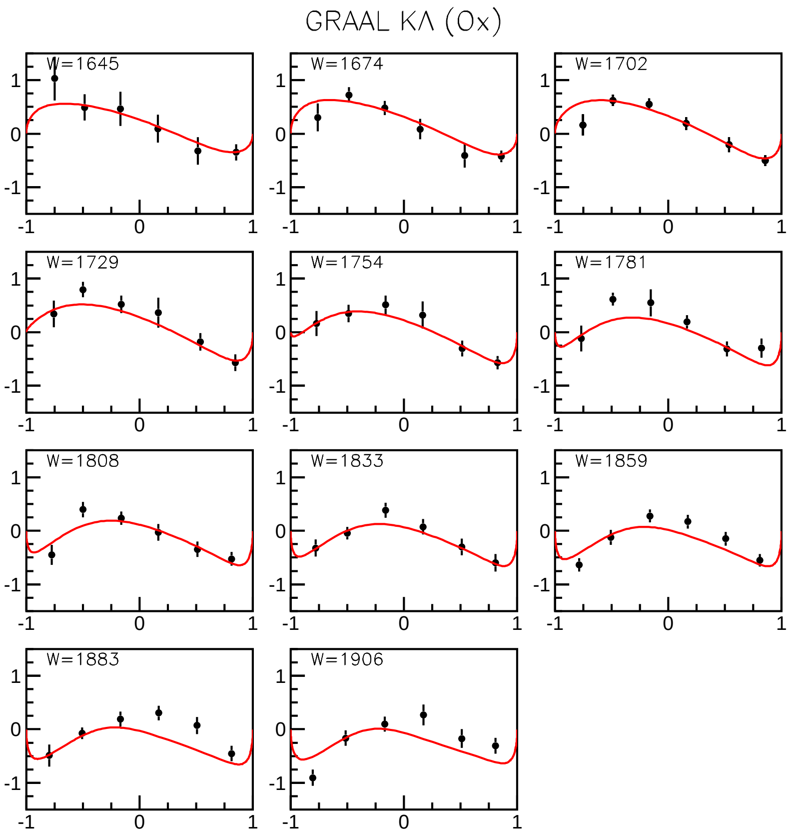

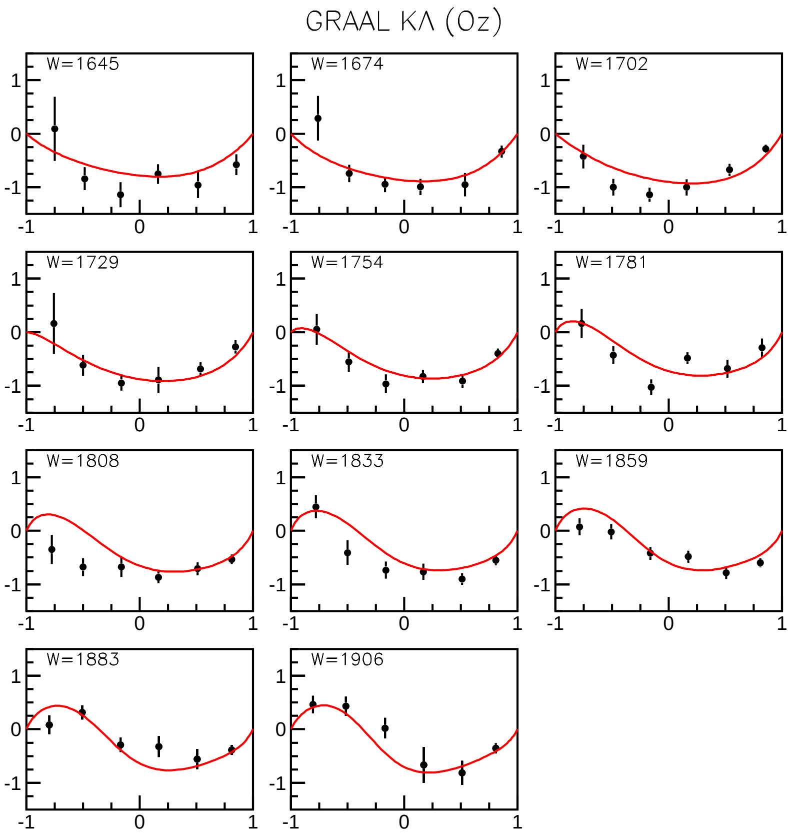

Summary

1. **An approach for the combined analysis of the pion and photo induced reaction with two and multiparticle final states is developed.**

2. **The combined analysis of more than 75 different reactions helped us to identify the properties of known baryons.**

3. **The new data support the two new baryon states observed in hyperon photoproduction of $P_{11}(1880)$ and $P_{13}(1900)$.**

4. **The η-photoproduction data reveal the baryon resonance $D_{15}(2070)$.**

5. **The $D_{33}(1940)$ state is needed for the description of the $\gamma p \to \pi^0 \eta p$ data.**

6. **The data on $\pi^- p \to \eta n$ and $\pi^- p \to K^0 \Sigma$ support an existence of $P_{11}(1710)$.**

7. **The spectrum of observed states is in direct contradiction with a classical quark model. The best explanations are chiral symmetry reconstruction or AdS/QCD soft-wall model (see talk of E.Klempt).**